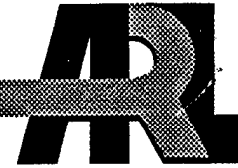


ARMY RESEARCH LABORATORY



Application of CFD to High Angle of Attack Missile Flow Fields

by Jubaraj Sahu, Karen Heavey,
and Surya Dinavahi

ARL-RP-3

September 2000

A reprint from the *American Institute of Aeronautics and Astronautics Atmospheric Flight Mechanics Conference*, no. AIAA 2000-4210, Denver, CO, August 2000.

Approved for public release; distribution is unlimited.

DTIC QUALITY INSPECTION
20001129 050

The findings in this report are not to be construed as an official Department of the Army position unless so designated by other authorized documents.

Citation of manufacturer's or trade names does not constitute an official endorsement or approval of the use thereof.

Destroy this report when it is no longer needed. Do not return it to the originator.

Army Research Laboratory

Aberdeen Proving Ground, MD 21005-5066

ARL-RP-3

September 2000

Application of CFD to High Angle of Attack Missile Flow Fields

Jubaraj Sahu and Karen Heavey
Weapons and Materials Research Directorate, ARL

Surya Dinavahi
Mississippi State University

A reprint from the *American Institute of Aeronautics and Astronautics Atmospheric Flight Mechanics Conference*,
no. AIAA 2000-4210, Denver, CO, August 2000.

Approved for public release; distribution is unlimited.

Abstract

Computational fluid dynamics (CFD) calculations have been performed for a missile body with and without fins. Numerical flow field computations have been made for various Mach numbers and roll angles using an unsteady zonal Navier-Stokes code (ZNSFLOW) and the chimera composite grid discretization technique at supersonic velocity and high angle of attack. Steady-state numerical results have been obtained and compared for cased modeling an ogive-cylinder missile with and without fins. Computed results show the details of the expected flow field features to include vortical crossflow separation. Computed results are compared with experimental data obtained for the same configurations and conditions and are generally found to be in good agreement with the data. The results help to show the predictive capabilities of CFD techniques for supersonic projectiles at incidence.

APPLICATION OF CFD TO HIGH ANGLE OF ATTACK MISSILE FLOWFIELDS

Jubaraj Sahu* and Karen R. Heavey

U.S. Army Research Laboratory
Aberdeen Proving Ground, MD 21005-5066

Surya Dinavahi
Mississippi State University

ABSTRACT

Computational fluid dynamics (CFD) calculations have been performed for a missile body with and without fins. Numerical flow field computations have been made for various Mach numbers and roll angles using an unsteady zonal Navier-Stokes code (ZNSFLOW) and the chimera composite grid discretization technique at supersonic velocity and high angle of attack. Steady-state numerical results have been obtained and compared for cases modeling an ogive-cylinder missile with and without fins. Computed results show the details of the expected flow field features to include vortical crossflow separation.

Computed results are compared with experimental data obtained for the same configurations and conditions and are generally found to be in good agreement with the data. The results help to show the predictive capabilities of CFD techniques for supersonic projectiles at incidence.

INTRODUCTION

The advancement of (CFD) has had a major impact on projectile design and development.¹⁻³ Improved computer technology and state-of-the-art numerical procedures enable solutions to complex, three-dimensional (3-D) problems associated with projectile and missile aerodynamics. In general, these techniques produce accurate and reliable numerical results for projectiles and missiles at

small angles of attack. Modern maneuvering projectiles and missiles are expected to experience moderate to large angles of attack during flight. Accurate determination of high angle of attack flow fields for these configurations is critical. The work presented in this paper was initiated as part of The Technical Cooperation Program (TTCP) effort aimed at assessing the capabilities of the Navier-Stokes solvers currently available to research scientists for high angle of attack flow fields.⁴ The TTCP research effort focused on the application of various computational techniques used in the areas of grid generation, algorithms, turbulence modeling and flow field visualization, and included participants from Canada, The United Kingdom, and the United States. Initially, these techniques were applied to a missile body at angle of attack. Subsequent efforts included computations for several finned missiles.⁵ Figure 1 shows a computational model used for one of the finned missiles.

The present research focuses on the application and assessment of the ZNSFLOW solver⁶ for high angle of attack flows. The product of a common high performance computing software support initiative (CHSSI) project, the ZNSFLOW code is a descendant of F3D, a program used successfully for many years on Cray vector processors such as the C90. Programming enhancements include the use of dynamic memory allocation and highly optimized cache management. ZNSFLOW is

* Aerospace Engineer, Associate Fellow AIAA

This work is declared work of the U.S. Government and is not subject to copyright protection in the United States.

highly portable and features a graphical user interface to facilitate problem setup. It has been used extensively in the computation of flow field calculations for projectile and missile programs of interest to the U.S. Army.⁷ The solver includes the Chimera overset discretization technique for CFD modeling of complex configurations.

The overset grid technique involves generating numerical grids about each body component and then oversetting them onto a base grid to form the complete model. With this composite overset grid approach, it is possible to determine the 3-D interacting flow field of the finned missile system and the associated aerodynamic forces and moments at different roll angles.

A description of the computational algorithm and the chimera technique is presented, followed by a description of the model geometry and computational grids used in the numerical computations. Results are shown for several missile configurations at supersonic speed and angle of attack. The results for the finned models include computations for two roll angle orientations. Computational data is compared with experimental data provided by the Defense Engineering and Research Agency (DERA) and the National Aeronautics and Space Administration (NASA).

SOLUTION TECHNIQUE

Governing Equations

The complete set of 3-D, time-dependent, generalized-geometry, Reynolds-averaged, thin-layer Navier-Stokes equations is solved numerically to obtain a solution to this problem and can be written in general spatial coordinates ξ , η , and ζ as follows:⁸

$$\partial_\tau \hat{q} + \partial_\xi \hat{F} + \partial_\eta \hat{G} + \partial_\zeta \hat{H} = R e^{-1} \partial_\zeta \hat{S}. \quad (1)$$

In Equation 1, \hat{q} contains the dependent variables: density, three velocity components, and energy. The thin layer approximation is used here, and the viscous terms involving velocity gradients in both the longitudinal and circumferential directions are neglected. The viscous terms are retained in the normal direction, ζ , and are collected into the

vector \hat{S} . These viscous terms are used everywhere. In the wake or the base region, similar viscous terms¹ are also added in the streamwise direction, ξ . An implicit, approximately factored scheme is used to solve these equations.

Numerical Algorithm

The implicit, approximately factored scheme for the thin-layer Navier-Stokes equations using central differencing in the η and ζ directions and upwinding in ξ is written in the following form:⁹

$$\left[I + i_b h \delta_\xi^b (\hat{A}^+)^n + i_b h \delta_\zeta \hat{C}^n - i_b h R e^{-1} \bar{\delta}_\zeta J^{-1} \hat{M}^n J \right. \\ \left. i_b D_i \downarrow_\zeta \right] \times [I + i_b h \delta_\xi^f (\hat{A}^-)^n + i_b h \delta_\eta \hat{B}^n \\ - i_b D_i \downarrow_\eta J \Delta \hat{Q}^n = -i_b \Delta t \{ \delta_\xi^b [(\hat{F}^+)^n - \hat{F}_\infty^+] \\ + \delta_\xi^f [(\hat{F}^-)^n - \hat{F}_\infty^-] + \delta_\eta (\hat{G}^n - \hat{G}_\infty) \\ + \delta_\zeta (\hat{H}^n - \hat{H}_\infty) - R e^{-1} \bar{\delta}_\zeta (\hat{S}^n - \hat{S}_\infty) \} \\ - i_b D_e (\hat{Q}^n - \hat{Q}_\infty), \quad (2)$$

in which $h = \Delta t$ or $(\Delta t)/2$ and the free stream base solution is used. Here, δ is typically a three-point second-order accurate central difference operator, $\bar{\delta}$ is a midpoint operator used with the viscous terms, and the operators δ_ξ^b and δ_ξ^f are backward and forward three-point difference operators. The flux \hat{F} has been eigensplit, and the matrices \hat{A} , \hat{B} , \hat{C} , and \hat{M} result from local linearization of the fluxes about the previous time level. Here, J denotes the Jacobian of the coordinate transformation. Dissipation operators D_e and D_i are used in the central space differencing directions.

Chimera Scheme

The chimera overset grid technique¹⁰⁻¹¹ involves generating independent grids about each body component and then oversetting them onto a base grid to form the complete model. This procedure reduces a complex body problem into a number of simpler subproblems. An advantage of the overset

grid technique is that it allows computational grids to be obtained for each body component separately and thus makes the grid generation process easier.

Because each component grid is generated independently, portions of one grid may lie within a solid boundary contained within another grid. Such points lie outside the computational domain and are excluded from the solution process. Equation 2 has been modified for chimera overset grids by the introduction of the flag i_b to achieve just that. This i_b array accommodates the possibility of having arbitrary holes in the grid. The i_b array is defined so that $i_b = 1$ at normal grid points and $i_b = 0$ at hole points. Thus, when $i_b = 1$, Equation 2 becomes the standard scheme, but when $i_b = 0$, the algorithm reduces to $\Delta \hat{Q}^n = 0$ or $\hat{Q}^{n+1} = \hat{Q}^n$, leaving \hat{Q} unchanged at hole points.

The set of grid points that form the border between the hole points and the normal field points are called inter-grid boundary points. These points are updated by interpolating the solution from the overset grid that created the hole. Values of the i_b array and the interpolation coefficients needed for this update are provided by a separate algorithm.¹⁰

Figure 2 shows an example where the missile body grid is a major grid and the fin grid is a minor grid. The fin grid is completely overlapped by the body grid, and thus its outer boundary can obtain information by interpolation from the body grid. Similar data transfer or communication is needed from the fin grid to the body grid. However, a natural outer boundary that overlaps the fin grid does not exist for the body grid. The overset grid technique creates an artificial boundary or a hole boundary within the missile grid that provides the required path for information transfer from the fin grid to the missile grid. The resulting hole region is excluded from the flow field solution in the missile body grid.

COMPUTATIONAL MODELS

The computational mesh for the missile body only case consists of a three-zone grid with a two-point overlap at the common boundaries. Initially, a one-million grid point case was used, consisting of 189 x 75 x 70 points in the axial, circumferential, and normal directions. The grid dimensions were increased to 375 x 180 x 140, creating a second grid of approximately 10-million

grid points. For the finned missile cases, a chimera gridding technique was used. A grid consisting of two zones was created for the missile body; the grids for the fins (two zones per fin) were obtained separately and attached to the body grids at different locations to create the desired configuration. Roll angles of 0 degrees and 45 degrees (+fin and xfin) were used. An overgrid covering the entire outer boundary completed the grid generation. The chimera technique makes the necessary interpolation for the areas where the grids overlap. Two DERA finned missile grids (+fin and xfin) were modeled, consisting of approximately 1.7 million grid points each. A more refined grid consisting of approximately 3.2 million grid points was used for the NASA (xfin) finned missile cases.

Boundary conditions are imposed explicitly. A no-slip condition was specified for the body surface for all configurations. The outer boundary of the overgrid was positioned far enough away from the projectile to be set at free stream conditions for the computations. The interpolation between the projectile grid and the overgrid is taken care of by the chimera routines. Likewise, the missile body grid to fin grid communication is also handled by the chimera routines. Because the free stream is supersonic, a simple flow field extrapolation is used for the downstream boundary condition. The symmetry of the missile allows the use of a symmetry boundary condition at 0 and 180 degrees, thus decreasing the number of required grid points by half.

RESULTS

Three-dimensional numerical computations have been performed for a 13-caliber ogive-cylinder missile configuration with and without fins, and at various Mach numbers, roll angles, and angles of attack. Because of the symmetrical properties of the geometry, the computations were performed on a half-model of each of the configurations, with appropriate boundary conditions imposed at the two symmetry planes in the circumferential direction. Computational results are compared with the experimental data obtained at DERA, U.K.¹² and at NASA Langley.¹³

A series of plots show comparisons of surface pressure coefficients. Results for the missile body configuration are shown in Figure 3. Three turbulence models were used: a Baldwin-Lomax algebraic model (BL), a Pointwise 1-equation model (1EQ), and a Pointwise 2-equation k-epsilon model (2EQ). Computations were done for both a one-million point grid and a 10-million point grid. The results shown here are for the 10-million grid point mesh. The agreement between the computational and experimental data is quite good along the ogive of the missile. In the cylinder region, there is excellent agreement on the windside of the projectile; however, the computational data on the leeside shows a marked variation compared to the experimental data. The computational results are quite similar for all three turbulence models used, with the 2-equation model showing slightly better results along the cylinder at $X/D = 8.5$ and 11.5 . Results for the one-million grid point solution are similar and are not shown here.

For the DERA finned missile configurations, circumferential surface pressure comparisons are shown at several axial (X/D) locations on the body surface as well as at various locations on the fins. For the +fin model, the agreement between experimental data and computed data at the axial locations shows moderate agreement on the windside and on the leeside (Figure 4), except at $X/D = 5.5$. The pressure comparisons on the fins are much better. Figures 5-7 show data for Y/D locations of 0.52, 0.81, 1.1 and 1.38 (root to tip) on each fin (positions a, c, e and g, respectively). The windward (bottom) fin shows good agreement at position a, while the comparisons show some variation at other wing positions. On the horizontal fin, there is some variation at position a (near the body-fin junction); otherwise, the computed surface pressures agree well with the experimental data on this fin. The surface pressures for the leeward (top) fin show moderate agreement near the body/fin junction, while there is good agreement at all other positions. The next series of plots (Figures 8-10) show similar comparisons for the xfin configuration. The surface pressure comparisons at the axial locations are generally good, except for the first axial position ($X/D=5.5$), where the agreement is poor on the leeside. However, the comparisons for both

fins are excellent. There is only a slight disagreement at positions a and c on the top fin near the body/fin junction. These computations were obtained using the Baldwin-Lomax turbulence model.

Computations for the NASA finned missile (x-configuration) were run for Mach numbers 1.6 and 2.7, at an angle of attack of 40 degrees, using both Baldwin-Lomax and 1-equation turbulence models. The results are shown in Figures 11-14. At Mach 1.6, the surface pressure predictions along the body of the missile are in good agreement with the experimental data, with the exception of the windward surface at $X/D=7.33$, the first X/D location on the fin. This is even more apparent for the Mach 2.7 case, at all X/D locations in the region of the fins. The computed surface pressures from both turbulence models show excellent agreement with the experimental data on the fins. The only exception is for Mach 2.7 at the Y/S location of 0.125, at the leading edge of the fin.

A limited amount of experimental pitot pressure data was available for the DERA configurations. Figures 15-17 show comparisons at several axial locations. In general, the computed results show the same flow features for the missile body alone cases. The agreement is not as good for the xfin missile configuration.

Tables 1-3 show computed force and moment coefficients for all cases. In general, there is excellent agreement between the experimental data and the computed values. There is a slight difference in the pitching moments (C_m) for the DERA finned missile.

Table 1. Force and Moment Data for DERA Body Only Missile Cases.

	EXP	1-MILLION POINT GRID			10-MILLION POINT GRID		
		BL	1EQ	2EQ	BL	1EQ	2EQ
C_N	1.95	1.85	1.83	1.86	1.83	1.82	1.87
C_m	4.61	4.68	4.91	4.93	5.08	4.97	4.99
C_A	0.19	0.20	0.24	0.22	0.20	0.23	0.21

Table 2. Force and Moment Data for DERA Finned Missile Cases.

	+FIN		xFIN	
	EXP	BL	EXP	BL
C_N	4.44	4.46	4.14	4.13
C_m	1.90	1.62	2.81	3.25
C_A	0.295	0.27	0.29	0.26

Table 3. Force and Moment Data for NASA Finned Missile Cases.

	MACH = 1.6			MACH = 2.7		
	EXP	BL	1EQ	EXP	BL	1EQ
C_N	21.3	21.4	21.0	19.6	20.4	19.4
C_m	8.0	8.9	9.2	4.0	3.9	4.1
C_A	n/a	0.8	0.9	n/a	1.0	1.0

CONCLUDING REMARKS

A time-marching Navier-Stokes code has been used to compute 3-D turbulent supersonic flow over a generic ogive-cylinder missile configuration, as well as two finned missile configurations. The computations were performed at various Mach numbers, angles of attack, and roll angles using ZNSFLOW, an updated version of the F3D code, and three different turbulence models: the Baldwin-Lomax algebraic turbulence model, a Pointwise one-equation model, and a Pointwise two-equation k-epsilon model. Comparisons of the computed surface pressures have been made with the experimental data provided by DERA and NASA. All three turbulence models predict the surface pressures very well on the ogive section of the missile. On the cylinder section, however, the comparison is not as favorable, especially on the leeward side. The surface pressure comparisons for the finned missile configurations are very good. Overall, there is excellent agreement between experiment and computation for both the DERA and NASA x-finned missiles. The DERA +fin missile shows some slight disagreement, but is generally quite good. Pitot pressure comparisons generally show the flow features observed in the experiment.

This work represents the application of a zonal Navier-Stokes solver using the chimera

overlapping grids approach for accurate numerical calculation of aerodynamics. The predictive numerical capability with various advanced turbulence modeling techniques provides the CFD community with quality tools with which to effectively perform computational research. It allows accurate numerical prediction of aerodynamic coefficients for projectile and missile configurations of interest to the military community.

REFERENCES

1. Sahu, J., "Numerical Simulations of Transonic Flows." *International Journal for Numerical Methods in Fluids*, vol. 10, no. 8, pp. 855-873, 1990.
2. Sahu, J., K. R. Heavey, and E. N. Ferry. "Computational Fluid Dynamics for Multiple Projectile Configurations." Proceedings of the 3rd Overset Composite Grid and Solution Technology Symposium, Los Alamos, NM, October 1996.
3. Sahu, J., K. R. Heavey, and C. J. Nietubicz. "Time-Dependent Navier-Stokes Computations for Submunitions in Relative Motion." Proceedings of the 6th International Symposium on Computational Fluid Dynamics, Lake Tahoe, NV, September 1995.
4. Sturek, W. B. "KTA-12: The Application of CFD to the Prediction of Missile Body Vortices." TTCP Final Report, June 1997.
5. KTA 2-15 Final Report, to be published.
6. Edge, H. L., et al. "Common High Performance Computing Software Support Initiative (CHSSI) Computational Fluid Dynamics (CFD)-6 Project Final Report: ARL Block-Structured Gridding Zonal Navier-Stokes (ZNSFLOW) Solver Software." ARL-TR-2084, February 2000.
7. Sahu, J., K. R. Heavey, D. M. Pressel, and S. Dinavahi. "Parallel Numerical Computations of Projectile Flow Fields." AIAA 17th Applied Aerodynamics Conference, Norfolk, VA, June 1999.
8. Pulliam, T. H., and J. L. Steger. "On Implicit

Finite-Difference Simulations of Three-Dimensional Flow." *AIAA Journal*, vol. 18, no. 2, pp. 159-167, February 1982.

9. Steger, J. L., S. X. Ying, and L. B. Schiff. "A Partially Flux-Split Algorithm for Numerical Simulation of Compressible Inviscid and Viscous Flows." Proceedings of the Workshop on CFD, Institute of Nonlinear Sciences, University of California, Davis, CA, 1986.

10. Steger, J. L., F. C. Dougherty, and J. A. Benek, "A Chimera Grid Scheme," *Advances in Grid Generation*, edited by K. N. Ghia and U. Ghia, ASME FED-5, June 1983.

11. Benek, J. A., T. L. Donegan, and N. E. Suhs, "Extended Chimera Grid Embedding Scheme With Application to Viscous Flows." AIAA Paper No. 87-1126-CP, 1987.

12. Birch, T. Personal communication.

13. Stallings, R.L., Jr., M. Lamb, and C. B. Watson. "Effect of Reynolds Number on Stability of Characteristics of a Cruciform Wing-Body at Supersonic Speeds." NASA Technical Paper 1683, 1980.

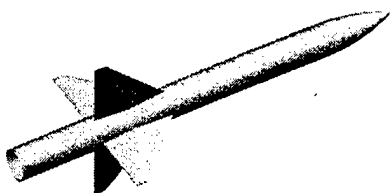


Figure 1. Computational model of NASA finned missile.

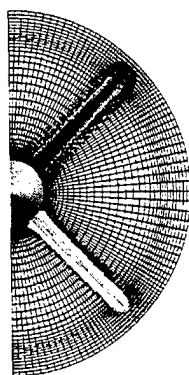


Figure 2. Computational grid showing chimera overlap.

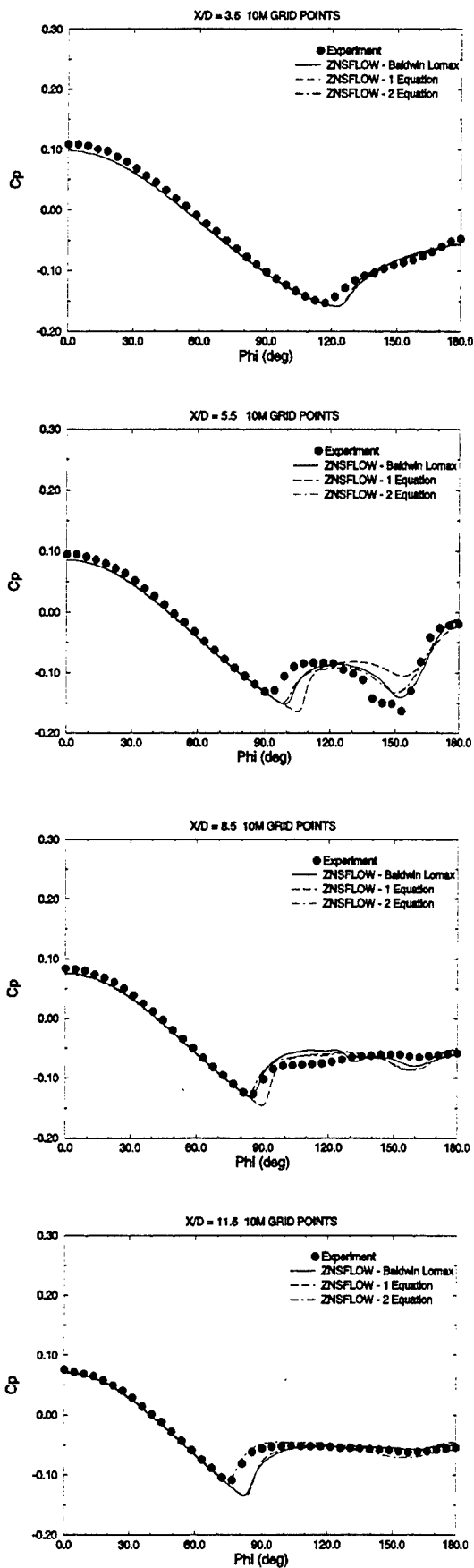


Figure 3. Surface pressure comparison at various axial locations, DERA body alone.

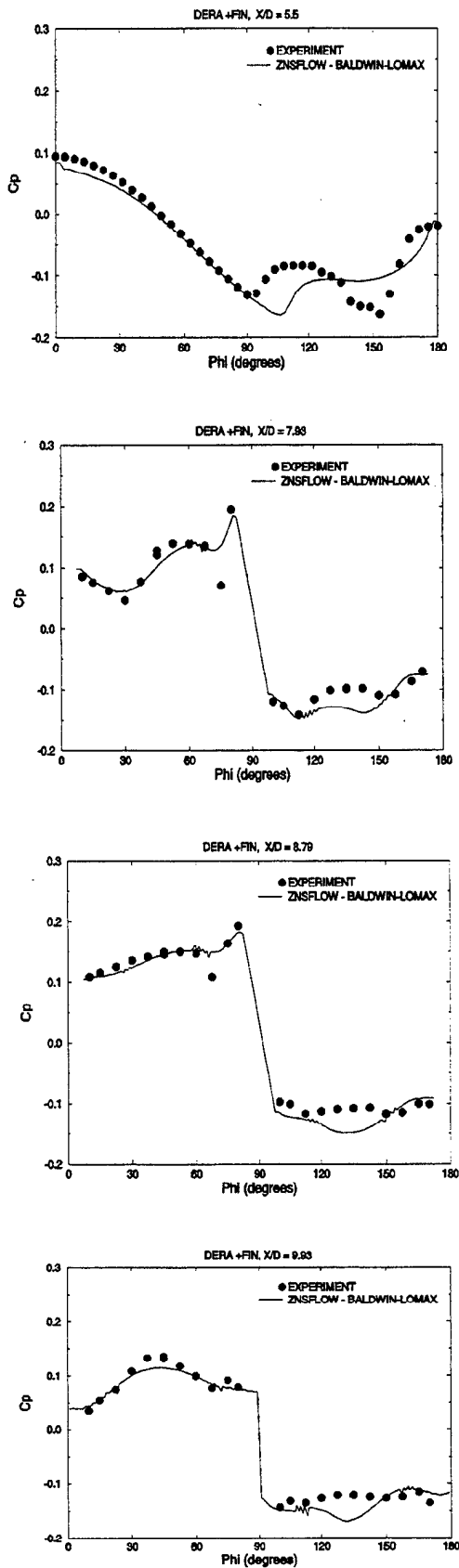


Figure 4. Surface pressure comparisons at various axial locations, DERA + fin.

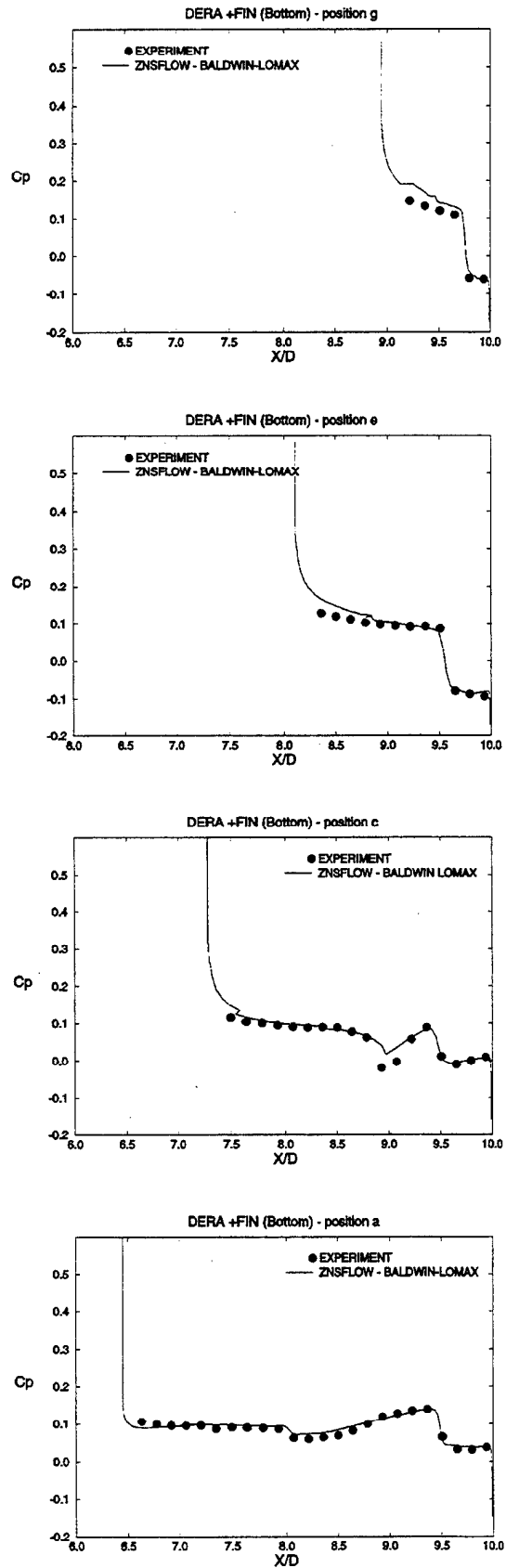


Figure 5. Surface pressure comparison on windward fin, various y/d , DERA + fin.

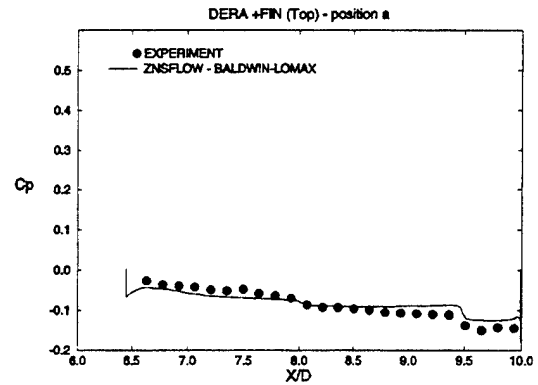
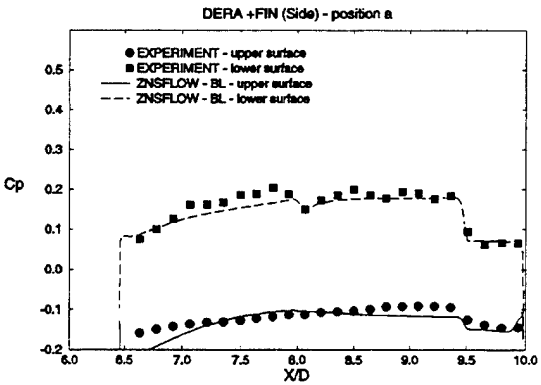
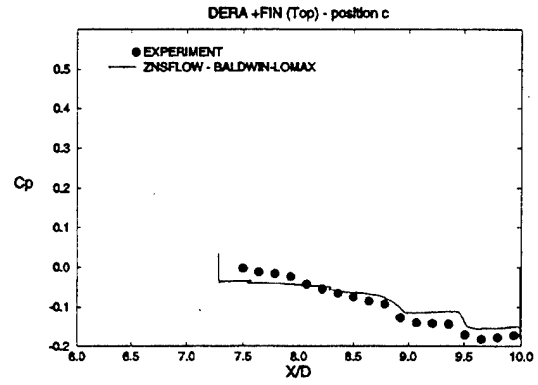
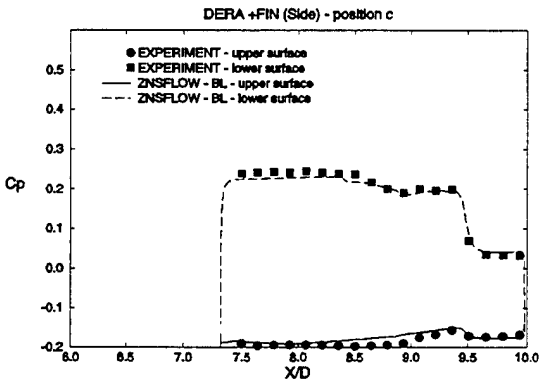
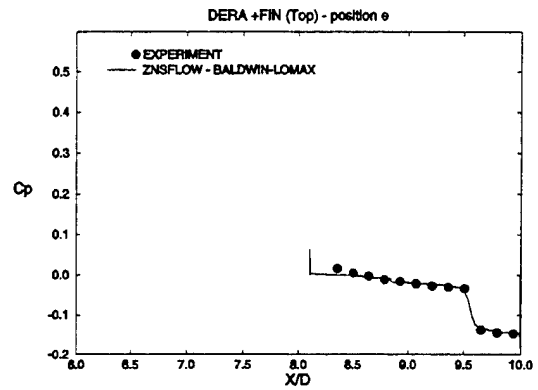
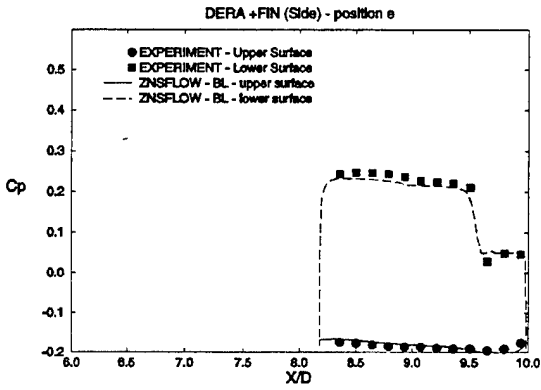
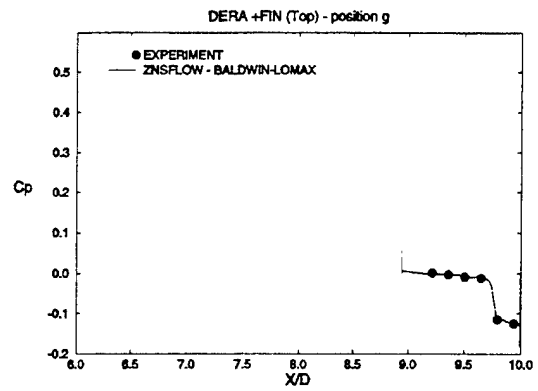
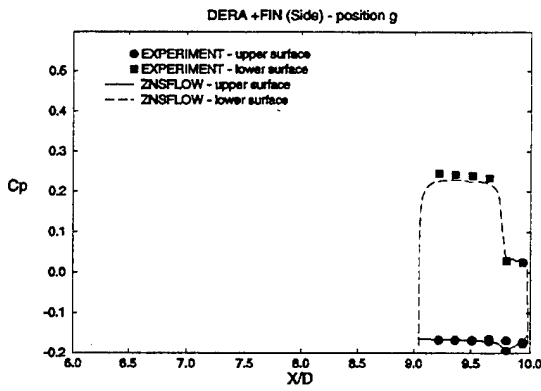


Figure 6. Surface pressure comparison on horizontal fin, various y/d , DERA +fin.

Figure 7. Surface pressure comparison on leeward fin, various y/d , DERA +fin.

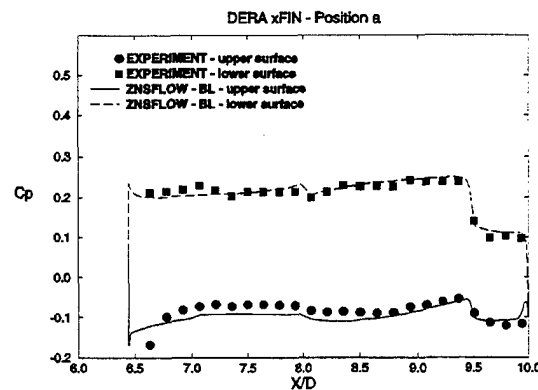
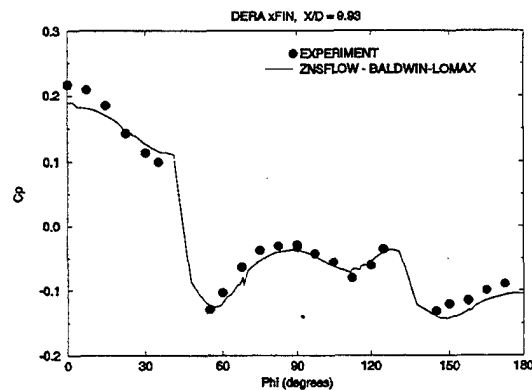
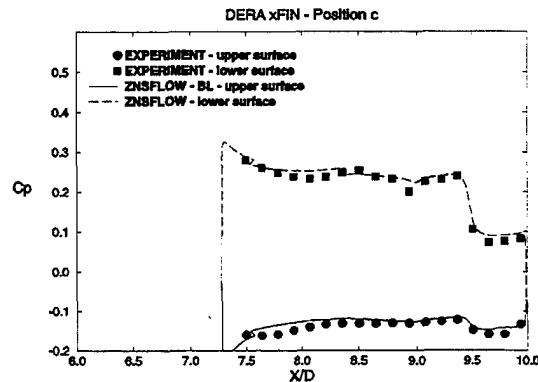
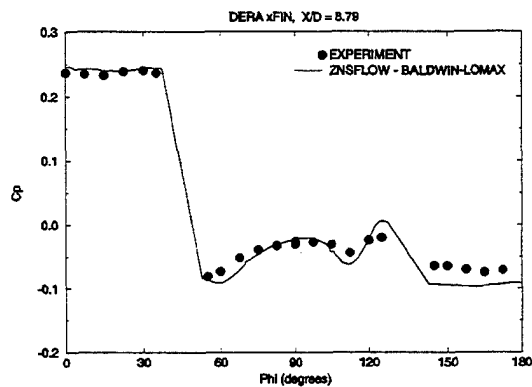
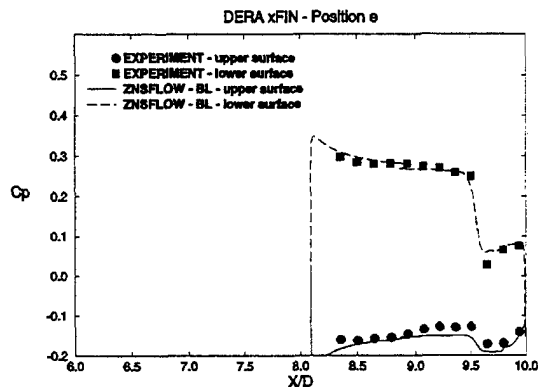
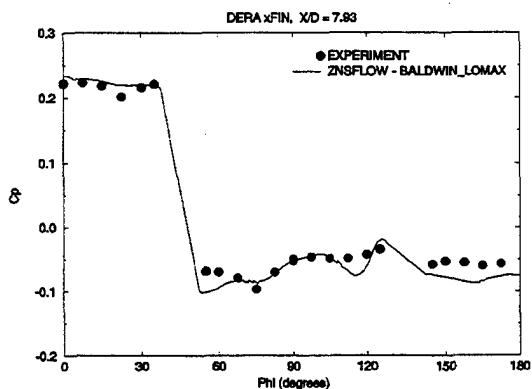
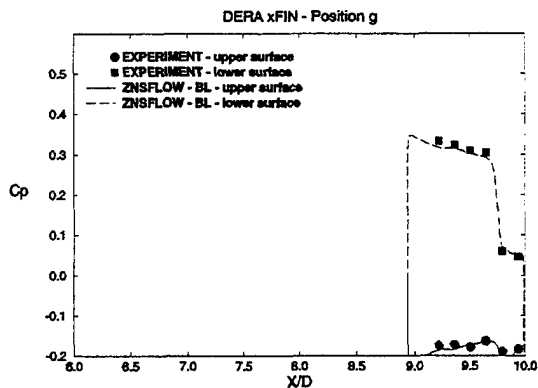
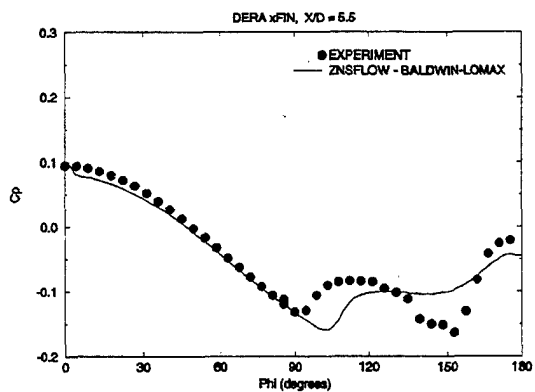


Figure 8. Surface pressure comparison at various axial locations, DERA xfin.

Figure 9. Surface pressure comparison on lower fin, various y/d locations, DERA xfin.

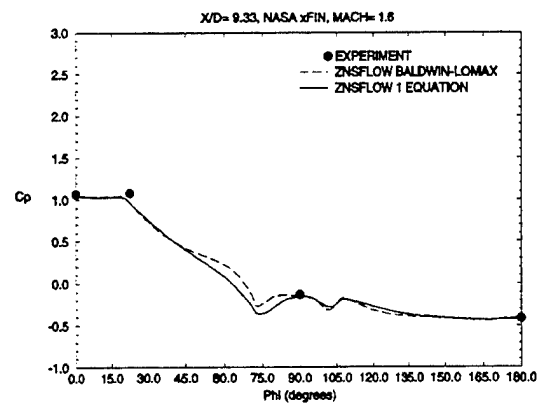
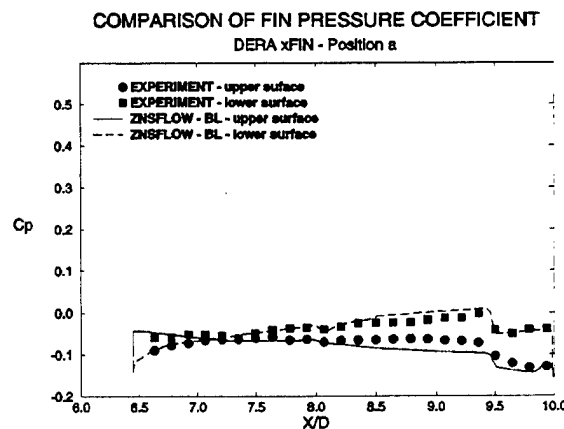
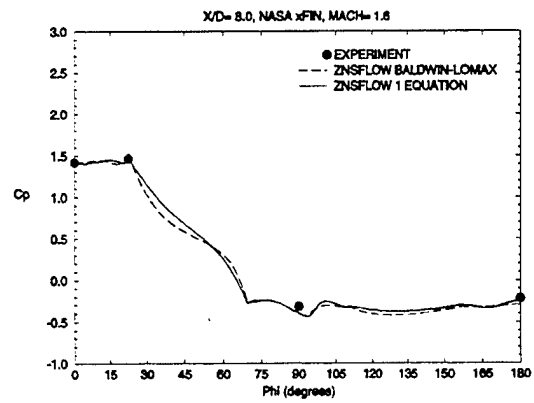
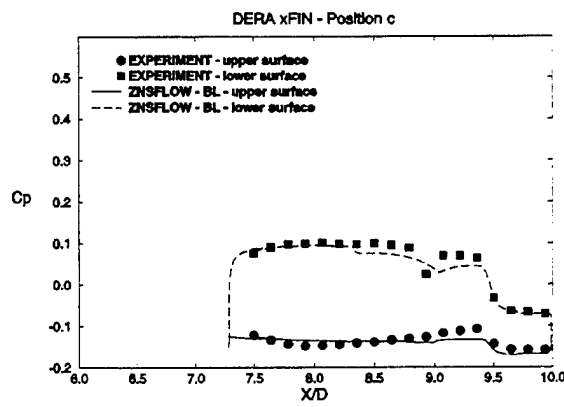
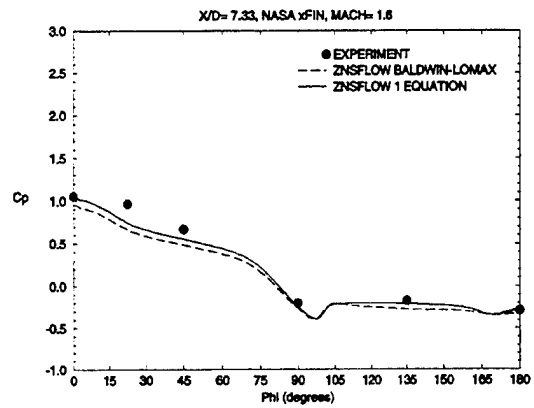
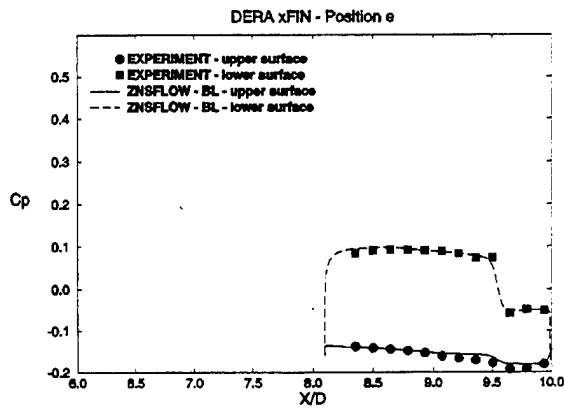
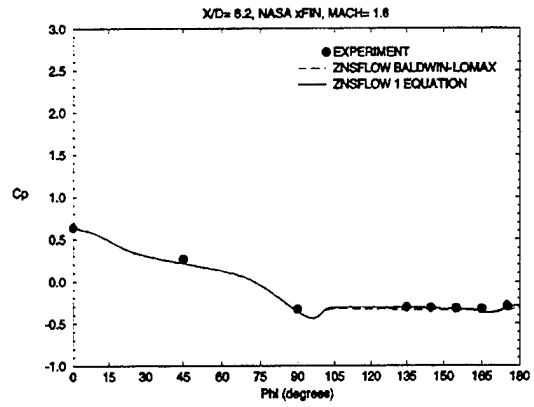
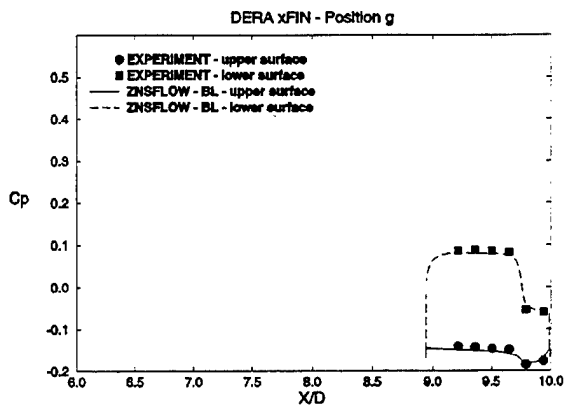


Figure 10. Surface pressure comparison on upper fin, various locations, DERA xfin.

Figure 11. Surface pressure comparison at various axial locations, NASA xfin.

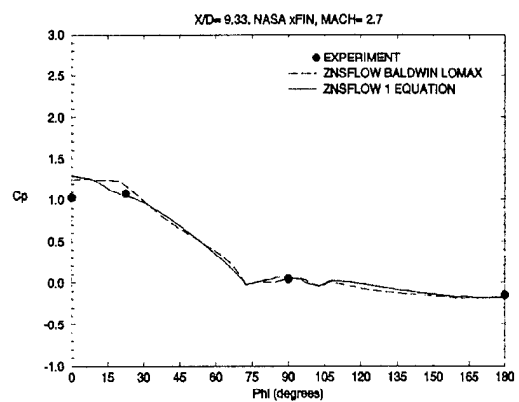
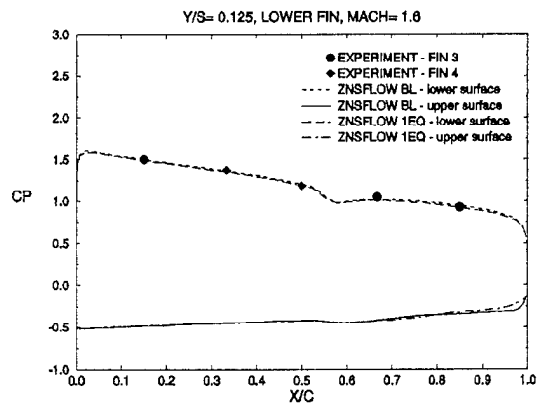
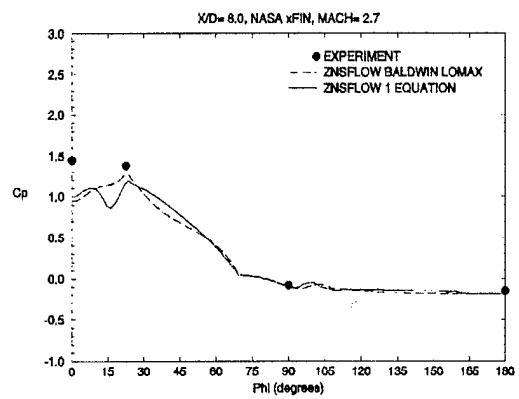
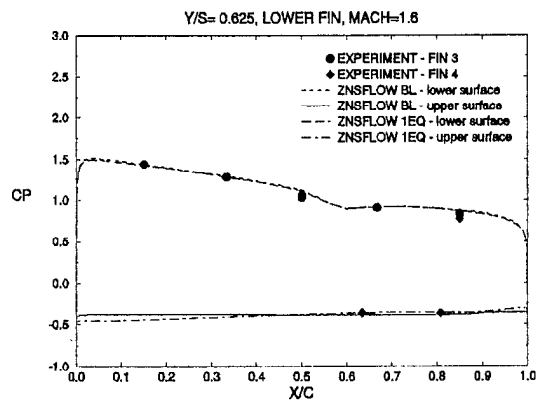
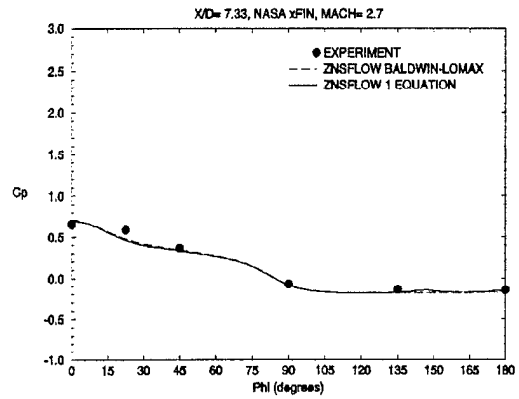
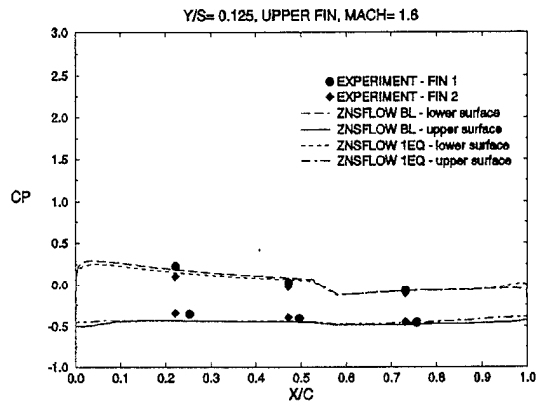
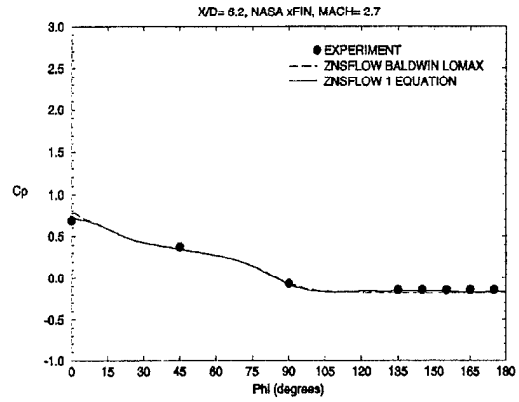
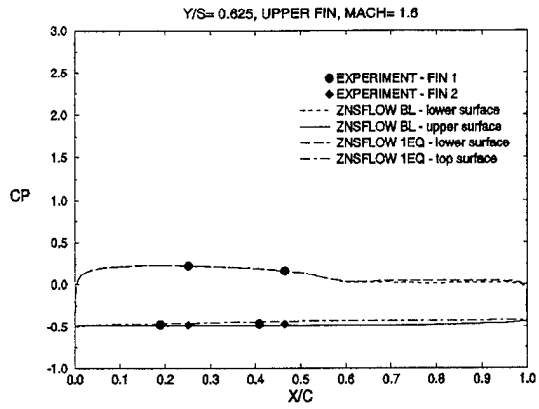


Figure 12. Surface pressure comparison for various y/s locations, NASA xfin.

Figure 13. Surface pressure comparison at various x/d locations, NASA xfin.

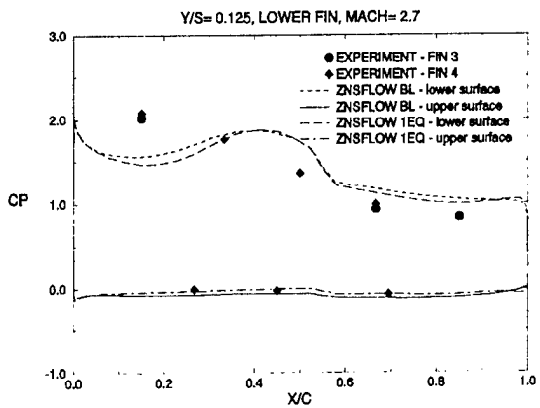
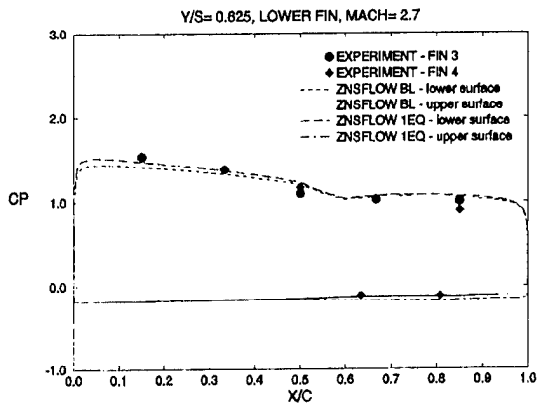
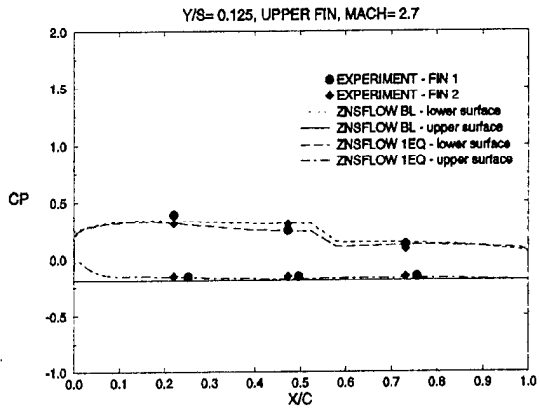
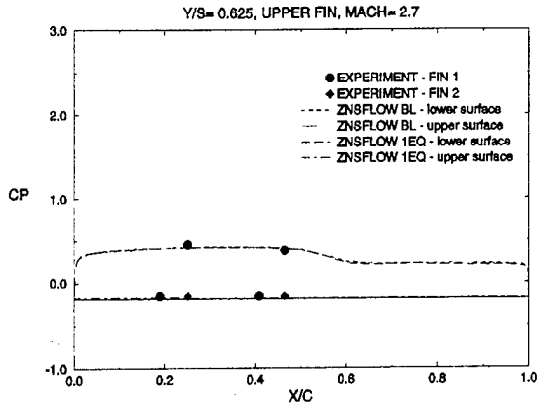


Figure 14. Surface pressure comparison at various y/s locations, NASA xfin.

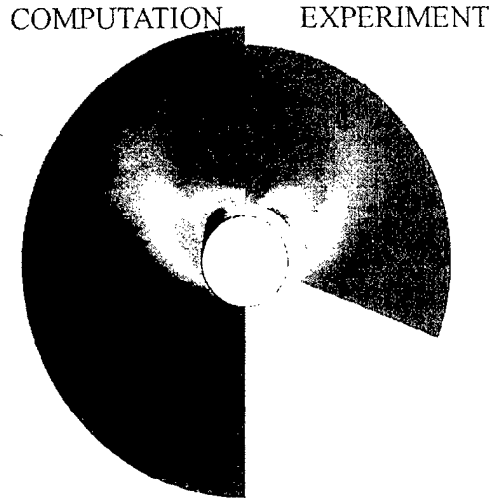


Figure 15. Pitot pressure comparison at $x/d=5.5$, DERA missile body alone.

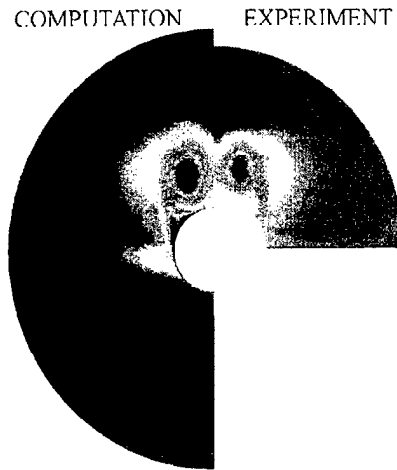


Figure 16. Pitot pressure comparison at $x/d=11.5$, DERA missile body alone.

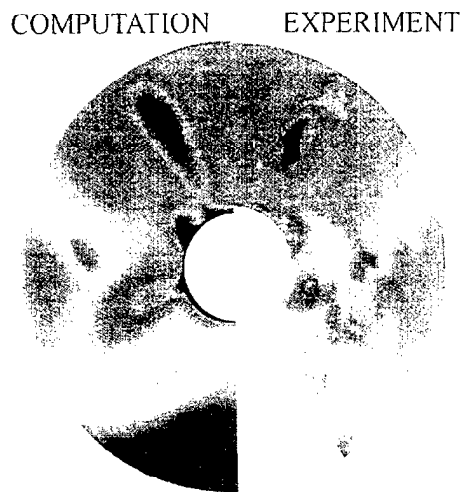


Figure 17. Pitot pressure comparison at $x/d=11.5$, DERA xfin.

<u>NO. OF COPIES</u>	<u>ORGANIZATION</u>	<u>NO. OF COPIES</u>	<u>ORGANIZATION</u>
2	DEFENSE TECHNICAL INFORMATION CENTER DTIC DDA 8725 JOHN J KINGMAN RD STE 0944 FT BELVOIR VA 22060-6218	1	DIRECTOR US ARMY RESEARCH LAB AMSRL D D R SMITH 2800 POWDER MILL RD ADELPHI MD 20783-1197
1	HQDA DAMO FDT 400 ARMY PENTAGON WASHINGTON DC 20310-0460	1	DIRECTOR US ARMY RESEARCH LAB AMSRL DD 2800 POWDER MILL RD ADELPHI MD 20783-1197
1	OSD OUSD(A&T)/ODDDR&E(R) R J TREW THE PENTAGON WASHINGTON DC 20301-7100	1	DIRECTOR US ARMY RESEARCH LAB AMSRL CI AI R (RECORDS MGMT) 2800 POWDER MILL RD ADELPHI MD 20783-1145
1	DPTY CG FOR RDA US ARMY MATERIEL CMD AMCRDA 5001 EISENHOWER AVE ALEXANDRIA VA 22333-0001	3	DIRECTOR US ARMY RESEARCH LAB AMSRL CI LL 2800 POWDER MILL RD ADELPHI MD 20783-1145
1	INST FOR ADVNCD TCHNLGY THE UNIV OF TEXAS AT AUSTIN PO BOX 202797 AUSTIN TX 78720-2797	1	DIRECTOR US ARMY RESEARCH LAB AMSRL CI AP 2800 POWDER MILL RD ADELPHI MD 20783-1197
1	DARPA B KASPAR 3701 N FAIRFAX DR ARLINGTON VA 22203-1714		<u>ABERDEEN PROVING GROUND</u>
1	NAVAL SURFACE WARFARE CTR CODE B07 J PENNELLA 17320 DAHLGREN RD BLDG 1470 RM 1101 DAHLGREN VA 22448-5100	4	DIR USARL AMSRL CI LP (BLDG 305)
1	US MILITARY ACADEMY MATH SCI CTR OF EXCELLENCE MADN MATH MAJ HUBER THAYER HALL WEST POINT NY 10996-1786	15	DIR USARL AMSRL WM BC J SAHU

INTENTIONALLY LEFT BLANK.

REPORT DOCUMENTATION PAGE

Form Approved
OMB No. 0704-0188

Public reporting burden for this collection of information is estimated to average 1 hour per response, including the time for reviewing instructions, searching existing data sources, gathering and maintaining the data needed, and completing and reviewing the collection of information. Send comments regarding this burden estimate or any other aspect of this collection of information, including suggestions for reducing this burden, to Washington Headquarters Services, Directorate for Information Operations and Reports, 1215 Jefferson Davis Highway, Suite 1204, Arlington, VA 22202-4302, and to the Office of Management and Budget, Paperwork Reduction Project(0704-0188), Washington, DC 20503.

1. AGENCY USE ONLY (Leave blank)		2. REPORT DATE September 2000	3. REPORT TYPE AND DATES COVERED Reprint, March 1999–April 2000	
4. TITLE AND SUBTITLE Application of CFD to High Angle of Attack Missile Flow Fields			5. FUNDING NUMBERS 1L1611102AH43	
6. AUTHOR(S) Jubaraj Sahu, Karen Heavey, and Surya Dinavahi*				
7. PERFORMING ORGANIZATION NAME(S) AND ADDRESS(ES) U.S. Army Research Laboratory ATTN: AMSRL-WM-BC Aberdeen Proving Ground, MD 21005-5066			8. PERFORMING ORGANIZATION REPORT NUMBER ARL-RP-3	
9. SPONSORING/MONITORING AGENCY NAMES(S) AND ADDRESS(ES)			10. SPONSORING/MONITORING AGENCY REPORT NUMBER	
11. SUPPLEMENTARY NOTES Mississippi State University, Mississippi State, MS 39762. A reprint from the <i>American Institute of Aeronautics and Astronautics Atmospheric Flight Mechanics Conference</i> , no. AIAA 2000-4210, Denver, CO, August 2000.				
12a. DISTRIBUTION/AVAILABILITY STATEMENT Approved for public release; distribution is unlimited.			12b. DISTRIBUTION CODE	
13. ABSTRACT (Maximum 200 words) Computational fluid dynamics (CFD) calculations have been performed for a missile body with and without fins. Numerical flow field computations have been made for various Mach numbers and roll angles using an unsteady zonal Navier-Stokes code (ZNSFLOW) and the chimera composite grid discretization technique at supersonic velocity and high angle of attack. Steady-state numerical results have been obtained and compared for cases modeling an ogive-cylinder missile with and without fins. Computed results show the details of the expected flow field features to include vortical crossflow separation. Computed results are compared with experimental data obtained for the same configurations and conditions and are generally found to be in good agreement with the data. The results help to show the predictive capabilities of CFD techniques for supersonic projectiles at incidence.				
14. SUBJECT TERMS computational fluid dynamics, finned missiles, chimera technique, high angle of attack, ZNSFLOW code			15. NUMBER OF PAGES 15	
			16. PRICE CODE	
17. SECURITY CLASSIFICATION OF REPORT UNCLASSIFIED	18. SECURITY CLASSIFICATION OF THIS PAGE UNCLASSIFIED	19. SECURITY CLASSIFICATION OF ABSTRACT UNCLASSIFIED	20. LIMITATION OF ABSTRACT UL	

INTENTIONALLY LEFT BLANK.

USER EVALUATION SHEET/CHANGE OF ADDRESS

This Laboratory undertakes a continuing effort to improve the quality of the reports it publishes. Your comments/answers to the items/questions below will aid us in our efforts.

1. ARL Report Number/Author ARL-RP-3 (Sahu) Date of Report September 2000

2. Date Report Received _____

3. Does this report satisfy a need? (Comment on purpose, related project, or other area of interest for which the report will be used.) _____

4. Specifically, how is the report being used? (Information source, design data, procedure, source of ideas, etc.) _____

5. Has the information in this report led to any quantitative savings as far as man-hours or dollars saved, operating costs avoided, or efficiencies achieved, etc? If so, please elaborate. _____

6. General Comments. What do you think should be changed to improve future reports? (Indicate changes to organization, technical content, format, etc.) _____

CURRENT
ADDRESS

Organization

Name

E-mail Name

Street or P.O. Box No.

City, State, Zip Code

7. If indicating a Change of Address or Address Correction, please provide the Current or Correct address above and the Old or Incorrect address below.

OLD
ADDRESS

Organization

Name

Street or P.O. Box No.

City, State, Zip Code

(Remove this sheet, fold as indicated, tape closed, and mail.)

(DO NOT STAPLE)

AD NUMBER	DATE 22 NOV 2000	DTIC ACCESSION
1. REPORT IDENTIFYING INFORMATION		REQUES: 1. Put your on revers 2. Complete 3. Attach for mailed to 4. Use uncl informa 5. Do not oi for 6 to
A. ORIGINATING AGENCY ARL-RP-3, "Application of CFD TO High Angle of Attack Missile Flowfields"		
B. REPORT TITLE AND/OR NUMBER		
C. MONITOR REPORT NUMBER		
D. PREPARED UNDER CONTRACT NUMBER		
2. DISTRIBUTION STATEMENT		DTIC: 1. Assign 2. Return
A		200001129 050

DTIC Form 50
JUL 96

PREVIOUS EDITIONS ARE OBSOLETE